

Interstellar heliospheric probe/heliospheric boundary explorer mission—a mission to the outermost boundaries of the solar system

**Robert F. Wimmer-Schweingruber · Ralph McNutt ·
Nathan A. Schwadron · Priscilla C. Frisch · Mike Gruntman ·
Peter Wurz · Eino Valtonen · The IHP/HEX Team**

Received: 29 November 2007 / Accepted: 11 December 2008 / Published online: 10 March 2009
© Springer Science + Business Media B.V. 2009

Abstract The Sun, driving a supersonic solar wind, cuts out of the local interstellar medium a giant plasma bubble, the heliosphere. ESA, jointly with NASA, has had an important role in the development of our current understanding of the Sun's immediate neighborhood. Ulysses is the only spacecraft exploring the third, out-of-ecliptic dimension, while SOHO has allowed us to better understand the influence of the Sun and to image the glow of

The IHP/HEX Team. See list at end of paper.

R. F. Wimmer-Schweingruber (✉)
Institute for Experimental and Applied Physics,
Christian-Albrechts-Universität zu Kiel,
Leibnizstr. 11, 24098 Kiel, Germany
e-mail: wimmer@physik.uni-kiel.de

R. McNutt
Applied Physics Laboratory, John's Hopkins University,
Laurel, MD, USA

N. A. Schwadron
Department of Astronomy, Boston University,
Boston, MA, USA

P. C. Frisch
University of Chicago, Chicago, USA

M. Gruntman
University of Southern California, Los Angeles, USA

P. Wurz
Physikalisches Institut, University of Bern, Bern, Switzerland

E. Valtonen
University of Turku, Turku, Finland

interstellar matter in the heliosphere. Voyager 1 has recently encountered the innermost boundary of this plasma bubble, the termination shock, and is returning exciting yet puzzling data of this remote region. The next logical step is to leave the heliosphere and to thereby map out in unprecedented detail the structure of the outer heliosphere and its boundaries, the termination shock, the heliosheath, the heliopause, and, after leaving the heliosphere, to discover the true nature of the hydrogen wall, the bow shock, and the local interstellar medium beyond. This will greatly advance our understanding of the heliosphere that is the best-known example for astrospheres as found around other stars. Thus, IHP/HEX will allow us to discover, explore, and understand fundamental astrophysical processes in the largest accessible plasma laboratory, the heliosphere.

Keywords ISM: general · Solar system: general · Interplanetary medium · Space vehicles: instruments · Cosmic rays

1 Introduction

After the exciting in-situ observations of the termination shock and the entry of the Voyager 1 spacecraft into the heliosheath (see Fig. 1), there is a growing awareness of the significance of the physics of the outer heliosphere. Its understanding helps to clarify the structure of our immediate interstellar neighborhood (e.g. [3]), contributes to the clarification of fundamental astrophysical processes like the acceleration of charged particles at a stellar wind termination shock (e.g., [15]) and beyond, and also sheds light on the question to what extent interstellar–terrestrial relations are important for the environment of and on the Earth [18, 41, 47]. In order to explore the boundary region of the heliosphere, it is necessary to send a spacecraft to perform advanced in-situ measurements particularly in the heliosheath, i.e. the region between the solar wind termination shock, and the heliopause, as well as in the (very) local interstellar medium. The Interstellar Heliopause Probe (IHP) will provide the first comprehensive measurements of key parameters of the local interstellar environment such as its composition, state, and magnetic field. Together with an accurate determination of the state of the heliospheric plasma across the heliosphere, these quantities are crucial to our understanding of how the heliosphere, and, much more generally, astrospheres, are formed and how they react to varying interstellar environments (Fig. 2).

Our current understanding of the interstellar medium and heliosphere is undergoing dramatic changes. Today, we understand the interstellar medium as a turbulent environment with varying degrees of ionization, highly variable composition and dust-to-gas ratio interacting with a complex magnetized and highly ionized heliospheric plasma—all in a complex background field of UV, cosmic rays, and neutral particles which is modified by the interaction itself. Thus, the heliosphere and its boundary regions serve as the worlds largest laboratory for complex plasmas.

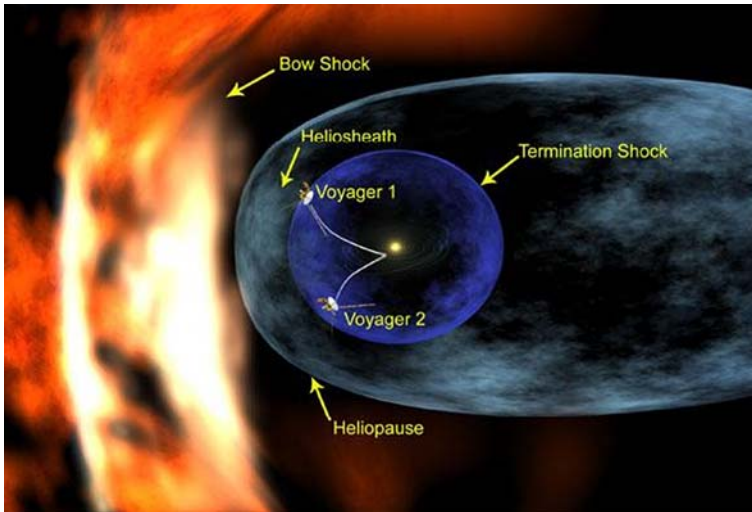


Fig. 1 Schematic view of the heliosphere depicting termination shock, heliosheath, heliopause, hydrogen wall, and bow shock

This complex region strongly modulates the flux of galactic cosmic rays which account for one half of the natural background radiation that life is exposed to on Earth [55] and shields Earth and solar system from highly reactive neutral hydrogen atoms, thus ensuring the habitability of Earth. How does this shielding function depend on the strongly varying interstellar environment? How does this shielding depend on the solar activity-induced heliospheric structure? What is the role of (anomalous) cosmic rays in these interstellar–terrestrial relations?

Fig. 2 During its history and orbit around the milky way, the solar system must have encountered a variety of interstellar environments (Image: HST)



2 Scientific objectives

2.1 Science goals

The Earth and the solar system are embedded in the vast interstellar medium out of which the Sun carves a large cavity, the heliosphere, by driving the solar wind. During its history, the solar system has moved through a variety of interstellar neighborhoods. Traversing these very different gas phases has consequences for the Earth and its environment which we are only today beginning to understand. The heliosphere serves as a shield against the changing interstellar neighborhood—yet our understanding of its structure and especially its boundaries is severely limited as is evident from SOHO, Ulysses, and Voyager measurements, as we will see in the discussion of question H4 (Fig. 3). In addition, the interstellar medium is the primeval material which the Sun, the planets, and ultimately terrestrial life were made of some 4.6 billion years ago, just as many other stars and planetary systems were formed at other times in different places. Exploring our local interstellar neighborhood will vastly enhance our understanding of the origin, formation, and evolution of stars, their planetary systems, and possibly of life. Thus, IHP addresses the three core Science goals described in Table 1.

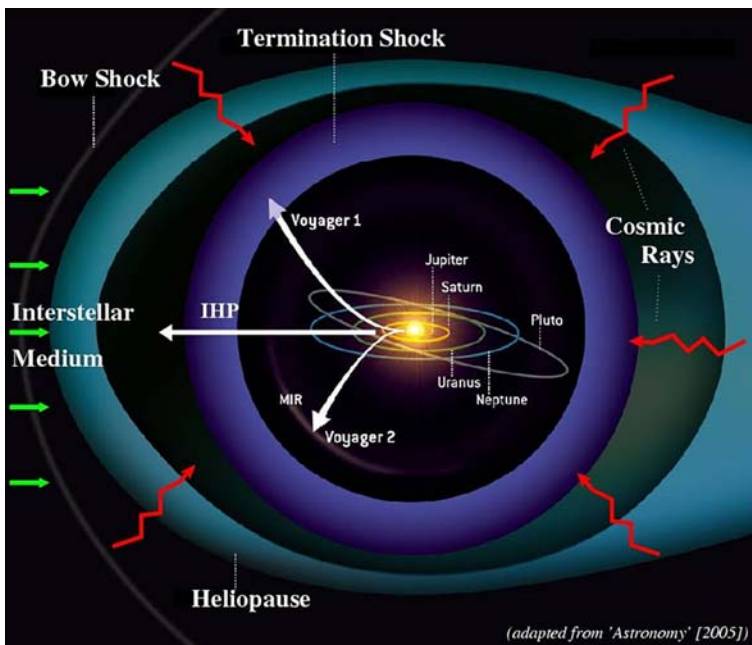


Fig. 3 The heliosphere is a gigantic plasma bubble cut out of the surrounding interstellar medium by the wind emitted by the Sun. It is the only accessible astrosphere and thus allows in-situ studies of fundamental physical and astrophysical processes

Table 1 IHP/HEX science goals

- H** How do solar wind and interstellar medium interact to form the heliosphere and how does this relate to the universal phenomenon of the formation of astrospheres?
- A** What are the properties of the very local interstellar medium and how do they relate to the typical ISM?
- F** How do plasma, neutral gas, dust, waves, particles, fields, and radiation interact in extremely rarefied, turbulent, and incompletely ionized plasmas?

In addition, due to its unique trajectory, IHP has the potential to address the puzzling Pioneer anomaly, resulting in a fourth, “bonus”, Science goal:

- B** What is the cause of the Pioneer Anomaly?

Current theoretical and modeling understanding of the heliosphere and its boundaries and interfaces is severely hampered by a lack of high-quality in-situ measurements. The only current data come from the ageing Voyager spacecraft, both launched in the 1970s. Their power is likely to last another 10 years which will allow them to reach a heliocentric distance not exceeding 130–140 AU. Comparison with Fig. 4 shows the likeliness that these spacecraft will not manage to measure the outer boundary regions of the heliosphere, the heliopause, hydrogen wall, and bow shock and will not be able to determine in-situ the properties of the local interstellar medium at all. To explore these regions is the primary science goal of IHP/HEX.

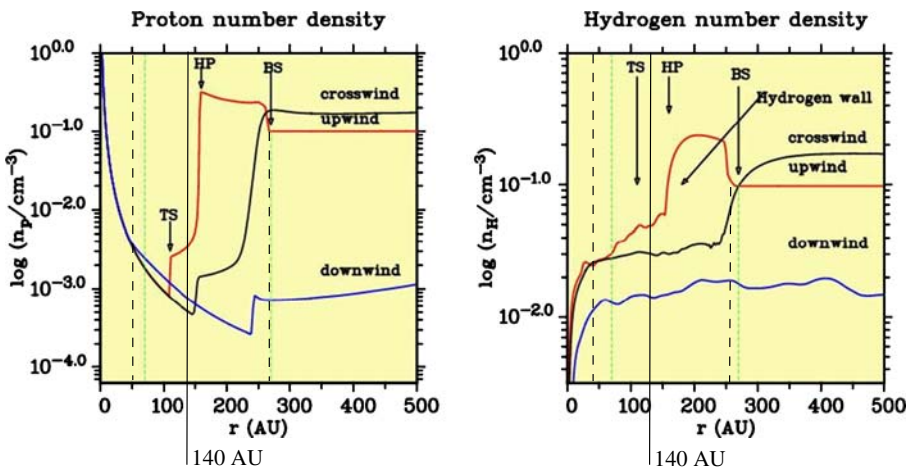


Fig. 4 Radial profiles of protons (*left*) and neutral hydrogen (*right*) in the upwind (*red*), the crosswind (*black*), and the downwind (*blue*) direction. The *vertical dashed lines* indicate the main discovery region of IHP, the *vertical solid line* denotes the maximum distance that the Voyager spacecraft will be able to investigate before their power runs out

2.2 H: How do solar wind and interstellar medium interact to form the heliosphere and how does this relate to the universal phenomenon of the formation of astrospheres?

Remarkably, the better we understand the physical processes at work on our Sun, the more we view our sun as a typical stellar object. The processes that give rise to our solar wind are clearly at work at other stars, possibly without exception. We are beginning to understand not only how the Sun heats its corona and powers the solar wind, but how these processes relate quite generally to stellar coronae and stellar winds. The heliosphere inflated by our solar wind is the direct analog to astrospheres inflated by the stellar winds of other stars. By studying other astrospheres, we may gain critical insights into the mass loss of other stars (Fig. 5). Further, the heliosphere, and astrosphere's more generally play a critical role in shielding out the majority of galactic cosmic radiation from the local interstellar medium. Galactic cosmic rays, in turn, strongly affect life on our planet, as detailed below.

2.2.1 H1: How does the heliosphere shield against cosmic rays and neutral particles and what role does it play in the interstellar–terrestrial relations?

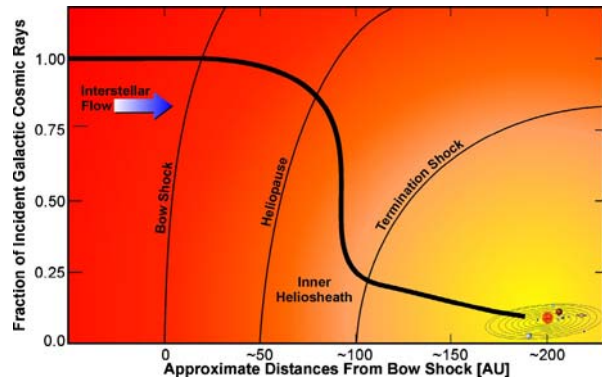
Cosmic rays are high energy charged particles which bombard Earth from above the atmosphere. Several thousand pass through a person's body every minute. These can cause biologic damage but also cause mutations which accelerate evolution.

The majority of GCRs present in interstellar space are shielded out by the outer heliosphere (Fig. 6), presumably via a strong magnetic barrier that forms

Fig. 5 An astrosphere has formed around a young star (image: Hubble)



Fig. 6 The fraction of incident GCRs on the heliosphere is most strongly reduced in the inner heliosheath where the slowdown of solar wind creates a large magnetic barrier to GCRs; this barrier is the dominant shield against GCR radiation in the solar system



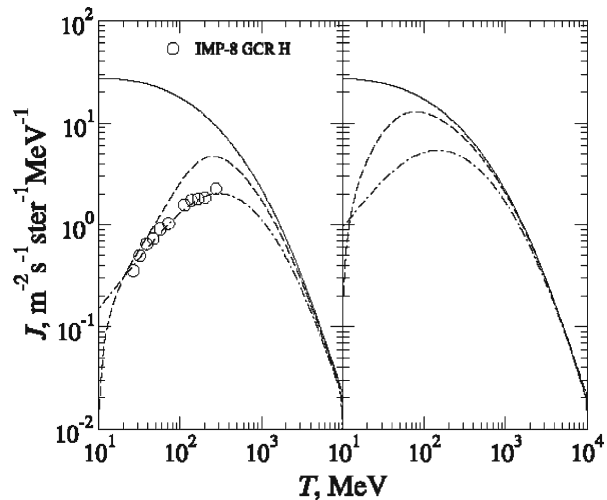
the inner heliosheath, where the solar wind slows prior to being deflected by the interstellar flow (e.g., [16]). Figure 6 shows the differential flux of GCRs from beyond the heliosphere to inside the heliosphere at 1 AU. A small fraction of GCRs penetrate into the heliosphere and propagate toward the Sun and planets. These residual GCRs are modulated by the solar wind's magnetic field in the inner heliosphere.

What we know about the dominant shielding of GCRs in the inner heliosheath region is very limited and based mostly on models and theory. It is nonetheless clear that the solar wind must slow down prior to meeting the interstellar flow. This slowdown must result in a strong pile-up of magnetic field since the magnetic field is frozen in to the solar wind. This magnetic barrier is believed to be the primary shield against GCRs entering the inner heliosphere (e.g., [16]).

Large changes in the LISM have dramatic effects on the heliosphere and the radiation environment of the solar system. For example, a typical enhancement in the density of the local interstellar medium by a factor of 10 causes the entire heliosphere to shrink to about a quarter of its current size [60], and increases the fluxes of GCRs at Earth by a factor of 2–6 [48]. Such large changes in the LISM have certainly occurred in the past and will occur again in the future [60].

Figure 7 shows the differential intensity of GCR protons, on the left for the present day, and on the right for a period when the heliosphere was smaller due to a larger density ($\times 10$) in the local interstellar medium. Shown are external boundary conditions [24], conditions near the terminations shock (dashed), and near Earth (dashed-dotted). Circles show IMP-8 data from [38]. The large increase in the levels of GCR radiation (right panel) reveals the critical influence of local interstellar conditions on the radiation environment of the solar system. The estimations made in Fig. 7 are purely theoretical. We do not currently have the observational knowledge required to understand how the local interstellar medium interacts with the heliosphere; observations of that global interaction are essential for understanding the radiation environment that must be traversed by astronauts for long missions to distant destinations, such as Mars.

Fig. 7 Galactic cosmic rays differential intensities in the heliosphere during the present day, *left*, and a future or past period when the heliosphere was smaller, with termination shock near 20 AU, due to a larger ($\times 10$) density in the interstellar medium [16]



On Earth, the radioisotope ^{10}Be provides a recent record of cosmic ray fluxes. The isotope is produced in Earth's upper atmosphere by spallation reactions of cosmic rays (CR) protons with energies higher than about 100 MeV and secondary neutrons with atmospheric nitrogen and oxygen. ^{10}Be records in Antarctic ice show two prominent peaks 35,000 and 60,000 years ago, when the radioisotope production rate was about twice the current value for about 1500 and 2000 years, respectively, which has been interpreted as due to supernovae in the vicinity of the heliosphere [45]. Could the GCR fluxes in the heliosphere change rapidly in the future due to changing conditions in the LISM? Again, the ^{10}Be record from ice cores can be used to show that at least in the past 300 years this has not been the case [2]. Nevertheless, because of the critical hazard posed by GCR radiation, future manned space travel will rely heavily on a better understand of the LISM's influence over the heliosphere, and the potential short and long term changes to the radiation environment.

2.2.2 H2: How do the magnetic field and its dynamics evolve in the outer solar system?

Figure 8 shows Voyager measurements of the expected compression of magnetic field at the termination shock. However, no sector boundaries were observed in the heliosheath during the first few months after the shock encounter, which could only be interpreted as due to a much lower convection speed (~ 17 km/s) of the local plasma relative to the spacecraft than expected. Further evidence for a significantly altered magnetic field in the downstream region comes from its fluctuations, which are much stronger in the heliosheath than in the heliosphere. Moreover, the statistical distribution of field magnitude changed [5] from lognormal (upstream) to Gaussian (downstream heliosheath), a transition that is not understood. This abrupt change in the nature

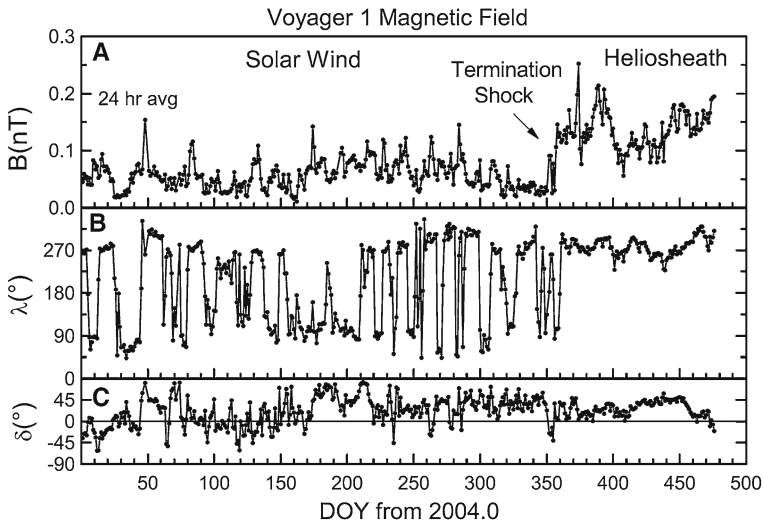


Fig. 8 Compression of the magnetic field across the termination shock [5]

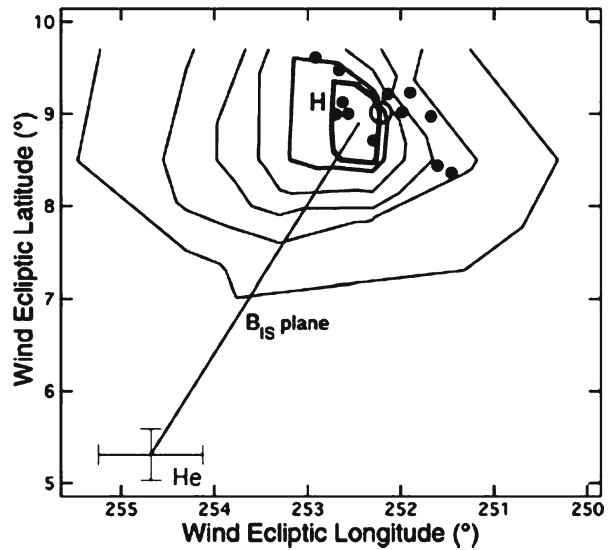
of the magnetic field across the termination shock has important consequences for the acceleration of particles at the termination shock, as these are affected by turbulent motions of the surrounding plasma. The level of low-frequency turbulence in resonance with the high-energy particles accelerated at the termination shock is unknown but key to understanding the modulation of galactic cosmic rays and the acceleration of anomalous cosmic rays.

2.2.3 H3: How do heliospheric structures respond to varying boundary conditions?

Observations by SWAN on SOHO have shown that the magnetic field in the very local interstellar medium lies at a significant angle to the galactic plane (Fig. 9) [32], a result recently independently confirmed with Voyager radio data [42]. On the other hand, general considerations about a galactic dynamo suggest that it should lie in the galactic plane at least on large scales. Thus, the very local field lies at a significant angle to the large scale field which is interpreted as a consequence of turbulent motions in the local interstellar cloud. Furthermore, the overabundance of carbon (see Science Objective A2) indicates an inhomogeneous local cloud. Together with observations of differences in flow angles, these observations imply an unexpected variability in the immediate interstellar vicinity of the heliosphere. Thus, we may expect that the heliosphere must react to these varying interstellar boundary conditions as well as to the solar-cycle variations at the inner boundary condition, the Sun.

Based on modeling efforts we expect that several heliospheric structures will react quite sensitively to changes in the interstellar medium [11]. Density fluctuations in the hydrogen wall should propagate around the heliosphere

Fig. 9 Observations with SOHO/SWAN indicate that the direction of the very local magnetic field is deflected from the average galactic plane direction by turbulent motions in the local interstellar cloud. From [32]



and thus give us a record of past variations in the heliosphere's very local interstellar neighborhood. The three-dimensional structure of the hydrogen density surrounding the heliosphere can be measured, thus giving us access to this archive.

Because we do not know the strength of the interstellar magnetic field, we do not know whether the heliosphere has a bow shock. The presence of a bow shock has important consequences for the turbulence in the outer heliosheath, i.e., between the bow shock and the heliopause. The shock generates downstream turbulence that translates into locally decreased spatial diffusion of energetic particles, thus contributing to a shielding against galactic cosmic rays. Furthermore, the trajectories of interstellar dust particles are altered by a bow shock, thus, the presence of a bow shock can be determined by a surprisingly simple measurement of the inflow direction of interstellar dust particles in a given mass range. Simulations [34] show that the flow direction of small particles is deflected by approximately 10° from the undisturbed direction when a sharp bow shock is present. Assuming that the inflow directions of gas and dust is the same, a measurement of the dust flow direction thus gives us the possibility to remotely detect the presence of a bow shock and, hence, indirectly determine a lower limit on the magnitude of the interstellar magnetic field.

2.2.4 H4: How do the boundary regions in the heliosphere modify the intensities of the various particle populations?

Early cosmic ray observers discovered an unusual subset of cosmic rays which consisted of singly ionized ions (instead of fully stripped nuclei) with energies of 1–50 MeV/nuc [40]. They were called Anomalous Cosmic Rays (ACRs). Most of the ACRs are species which have high ionization thresholds, such

as He, N, O, Ne, and Ar. Until recently, ACRs were thought to arise only from neutral atoms in the interstellar medium [14] that drift freely into the heliosphere through a process that has four essential steps: first, there is a source of neutral particles, traditionally thought to be only interstellar neutral atoms that stream into the heliosphere; second, the neutrals are converted into ions, called pickup ions since they are picked up and swept out by the solar wind; third, pickup ions are pre-accelerated by shocks and waves in the solar wind (see also [50]); and finally, they are accelerated to their final energies at the termination shock [43] or beyond it. Easily ionized elements such as C, Si, and Fe are expected to be strongly depleted in ACRs since such elements are not neutral in the interstellar medium and therefore cannot drift into the heliosphere.

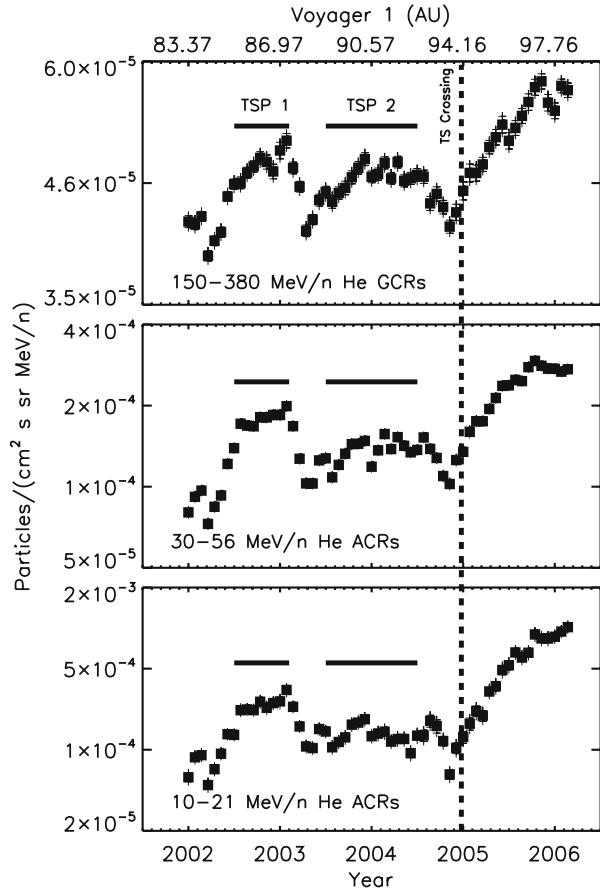
Due to instruments like SWICS on Ulysses, we have been able to detect pickup ions directly, and due to ongoing measurements by cosmic ray detectors on spacecraft such as Voyager and Wind, researchers have been able to detect unusual components of the ACR [8, 35, 46]. There is a growing understanding that, in addition to the traditional interstellar source, grains produce pickup ions throughout the heliosphere: grains near the Sun produce an “inner source” of pickup ions, and grains from the Kuiper Belt provide an “outer” source of pickup ions and anomalous cosmic rays (see, e.g., [49], and references therein.).

Not only are recent observations calling into question the sources of ACRs, but also the very means by which they are accelerated. The prevailing theory until V1 crossed the TS was that pickup ions were energized at the TS to the 10–100 MeV energies observed [43]. Figure 10 shows the strong correlation between modulated ACR and GCR helium in the vicinity of the termination shock. The data points show V1 observations [39] from Jan 2002 to Feb 2006, with 150–380 MeV/nuc GCRs in the top panel and 30–56 and 10–21 MeV/nuc ACRs in the middle and bottom panels. As is obvious in the figure, when V1 crossed the TS, it did not see a peak in the ACR intensity as the aforementioned theory predicted [53]. Instead the ACR intensities continued to increase in the heliosheath. One suggestion is that the ACRs are accelerated in the flanks of the heliosheath and the source region is not observed by V2 near the nose [37]. Another suggestion is that the acceleration region was affected by a series of merged interaction regions (MIRs, e.g., [6]) before the V1 crossing which diminished the acceleration process [15, 39], in which case V2 may see a different ACR profile when it crosses the TS. Yet other explanations have been offered, however, there is currently no consensus on any one explanation.

2.2.5 H5: How does the interstellar medium affect the outer solar system?

Interstellar dust entering the heliosphere interacts with the small planetary objects that are located beyond the orbits of the giant planets of our solar system. This region is believed to consist of remnants of planetesimals that were formed in the protoplanetary disk and studying the small objects in this trans-Neptunian regions is of basic interest for comparing the solar system to

Fig. 10 The time evolution of Anomalous Cosmic Rays (bottom two panels) and Galactic Cosmic Rays (top panel) observed by Voyager 1



extra-solar planetary systems. The flux of the interstellar dust is considered as a source of dust production by impact erosion in this trans-Neptunian region [59] and also limits the lifetime of the outer solar system dust cloud.

A signature of this interaction may have been found in the ACR. Recent observations from the Voyager and Wind spacecraft have resolved ACR components comprised of easily ionized elements (such as Si, C, Mg, S, and Fe; [8, 35, 46]). An interstellar source for these “additional” ACRs, other than a possible interstellar contribution to C, is not possible [8]. Thus, the source for these ACRs must reside within the heliosphere. There are a number of potential ACRs sources within the heliosphere [49] which are all easily ruled out. It is currently believed that the additional population of ACRs requires a large source of pickup ions inside the heliosphere that is produced far beyond 1 AU. Schwadron et al. [49] suggest that there exists a strong outer heliospheric source of pickup ions that explains the presence of easily ionized ACRs. The source is material extracted from the Kuiper belt through a series of processes (shown schematically by the blue lines in Fig. 11): First, micron-sized dust

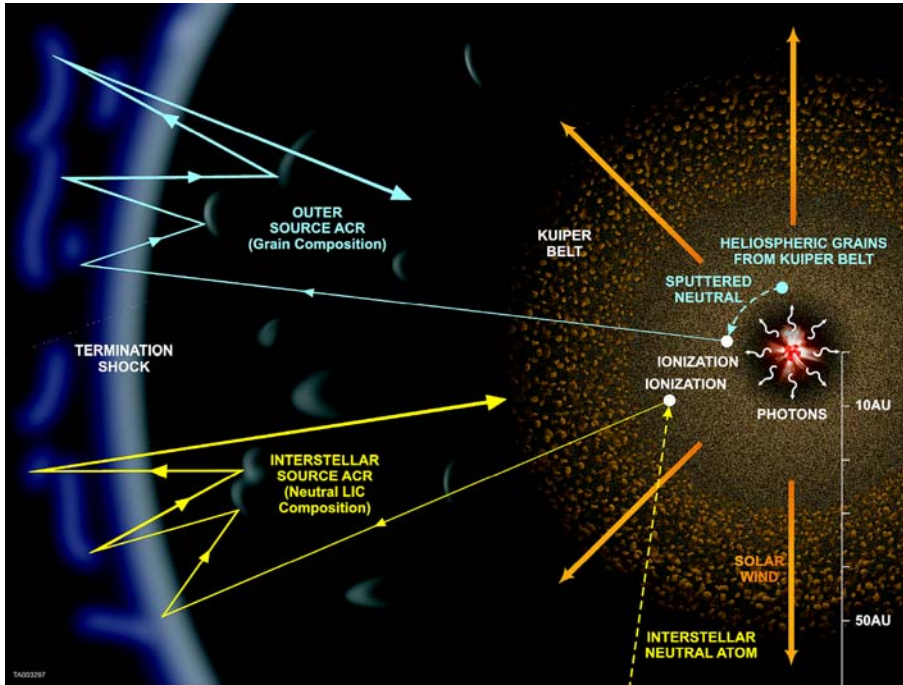


Fig. 11 An illustration of ACR production [49]. Yellow curves apply to the known interstellar source ACRs (adapted from [26]), while blue curves apply to the outer source, described later in the paper

grains are produced due to collisions of objects within the Kuiper Belt¹; grains spiral in toward the Sun due to the Poynting–Robertson effect (see [7]); neutral atoms are produced by sputtering and are converted into pickup ions when they become ionized; the pickup ions are transported by the solar wind to the termination shock and, as they are convected, are pre-accelerated due to interaction with shocks and due to wave–particle interactions; finally, they are injected into an acceleration process at the termination shock to achieve ACR energies.

2.3 A: What are the properties of the very local interstellar medium and how do they relate to the typical ISM?

2.3.1 A1: What is state and origin of the local interstellar medium?

The Local Interstellar Cloud (LIC) belongs to a flow of low-density ISM embedded in the very low density and hot ($T \sim 10^6$ K) Local Bubble (LB, see

¹And possibly by interstellar dust grains which limit the lifetime of these dust grains, see previous paragraph.

Fig. 12 The present day temperature distribution and extension of the Local Bubble (labeled LB) and the Loop I superbubble (L1) in a section through the galactic midplane about 14.5 million years after their origin. The solar system is located at the intersection of the various lines-of-sight (solid lines in the Figure) in the LB [3]

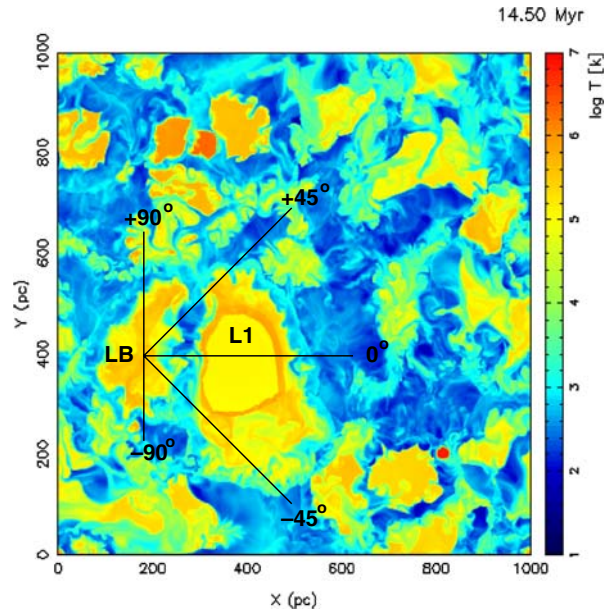


Fig. 12). The bulk motion of this cluster of interstellar clouds points toward the center of the Loop 1 super-bubble (L1). Within this overall flow, distinct cloudlets have been identified with unique velocities. The motional direction of the cloud currently feeding interstellar gas into the heliosphere has been determined with the GAS experiment on Ulysses [56] and, interestingly, is not aligned with the overall motion—it appears to be 1.5 km/s slower than the observed ISM velocity towards α -Cen. This suggests that the heliosphere is at or close to the edge of the LIC and, thus, the material surrounding the heliosphere could change on time scales as short as the duration of IHP (see, e.g., [18], for a review). Studies of the orientation of the local interstellar field also appear to indicate the importance of a highly turbulent interstellar flow (see Science Objective A4). The associated timescales are comparable to the present duration of space age and our understanding of the importance of the heliosphere in shielding us from the interstellar medium. For instance, neutron-monitors, first introduced in 1957 with the International Geophysical Year, have shown that the galactic cosmic ray intensity at Earth varies with solar activity. Galactic cosmic rays produce the important climate tracer ^{14}C by spallation of nitrogen in the Earth's atmosphere. We currently base much of our modeling efforts for climate physics on uncertain understanding of the relation between GCR-produced ^{14}C and solar activity based on historic records of sunspots. Given that one of the time scales of the the variability of the interstellar boundary conditions is roughly the same as the time scale as the neutron monitor data or maybe the sunspot record, the question naturally arises whether the naive assumption that the modulation of GCR by the heliosphere is only determined by solar activity may not be overly simplified.

Heliospheric structure and modulation is determined by time-varying boundary conditions at the Sun and in the local interstellar medium.

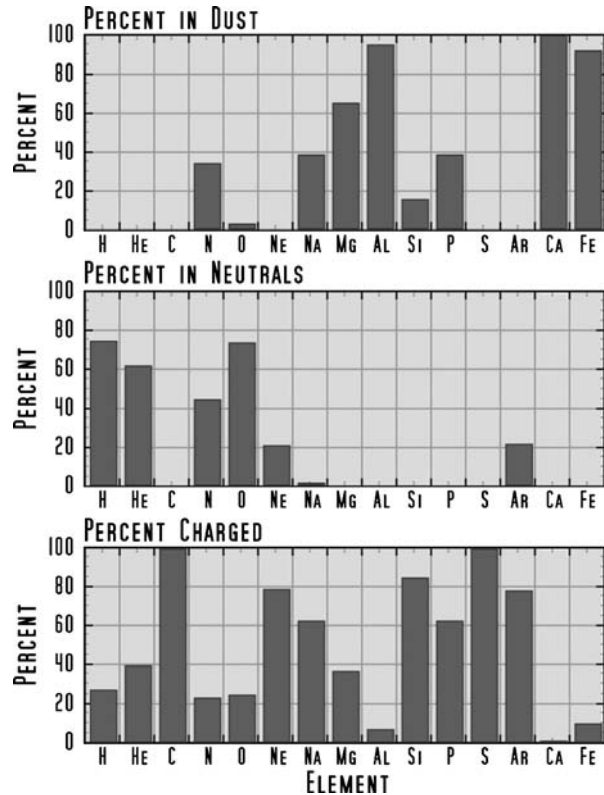
2.3.2 A2: *What is the composition of the local interstellar medium?*

Compositional studies have established themselves an extremely successful tool to understand the origin and evolution of astronomical and solar system bodies. Based on studies of the solar system, we believe that the central star and its planets are made of the same material with only small compositional gradients in similarly behaving elements across the planetary system (if any at all). The driving fractionation processes are condensation and heating. Similar studies of galactic composition and its evolution are hampered by these often neglected but important processes. Frequently, the composition of the ISM can only be determined in the gas phase using, e.g., absorption lines. The missing elements (relative to a “universal” galactic composition, derived from solar composition) are then thought to be locked into interstellar dust grains. The composition of dust is very hard to measure remotely, some progress has been made using measurements of extinction, polarization and emissivity over a wide range in wavelengths. However, the effects of space weathering on individual dust particles is hardly understood and accounted for. Thus, it is safe to say that the composition of the interstellar medium is only understood in a qualitative way (Fig. 13).

To make the next step to quantitative understanding of the composition in the galaxy, we need to understand this critical process. The only accessible interstellar cloud is the local cloud, and, hence, we need to measure its composition in the dust, gas, and plasma phase. A key ingredient in this respect is the dust-to-gas mass ratio which is different when measured in the LIC and in-situ in the heliosphere. Radiation pressure, solar gravity, and Lorentz forces modify the flux of the dust into the solar system and the acting forces vary with the dust properties as well as with the plasma and magnetic field conditions (see, e.g., [17, 22], for a review). As a result, both the dust fluxes in the interstellar medium and in the outer solar system, and, hence, the corresponding dust-to-gas mass ratios, are estimated with great uncertainty, because the small particles, which probably make up the majority of the dust number density, are deflected at the boundaries of the heliosphere [9]. The in-situ heliospheric measurements are affected by solar activity and polarity and the detailed structure of the heliospheric interfaces, hence measuring the time dependence of this ratio gives important information on the latter boundaries and on the properties of interstellar dust.

A further key measurement will be the abundance of certain abundant elements in the VLISM and comparison with measured abundances of interstellar ions (in the form of pickup ions) and atoms (in the form of neutral gas) within the heliosphere. Understanding the filtration effects on various elements will allow us to generalize them to other elements and thus to finally derive the elemental abundances in the very local interstellar medium from in-situ measurements within the heliosphere. The measurement of the abundances of

Fig. 13 The relative contributions to the interstellar medium from dust, neutrals, and plasma components

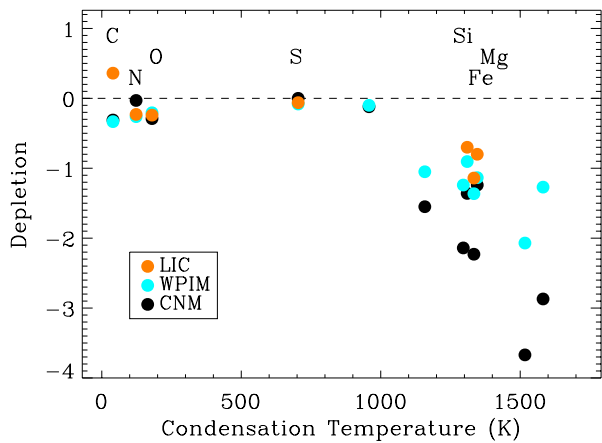


elements in the LIC can only be done if we can measure the ionization state of hydrogen (or of oxygen (or N) because it readily charge exchanges with H). This is the most prominent hurdle in establishing the metallicity of the LIC (Fig. 14).

This becomes even more important if we want to compare the local interstellar composition with that of the solar system. Intriguingly, we observe that the Sun (and solar system) appear to be isotopically heavier than the interstellar medium at a similar galactocentric distance. This is currently the only indication that the solar system must have migrated several kiloparsec within its galactic environment. In other words, studying the differences between solar system and galactic abundances is the only opportunity we have to quantitatively assess the effects of galactic dynamics.

A further puzzle is the carbon abundance of the LIC. In interstellar space the C abundance is a factor of about 2.5 below solar abundances in the gas phase, and, as discussed above, the missing carbon is thought to be locked up in interstellar dust grains or giant molecules consisting of PAH's. In the LIC, C appears to be significantly *overabundant* in the gas-phase for reasons not understood [51]. This appears to indicate not only total destruction of carbonaceous dust grains locally, but also inhomogeneous mixing of gas and

Fig. 14 Compositional patterns for the local interstellar environment. *Orange symbols* show LIC composition from model 26 of [52], *cyan symbols* show warm partially ionized matter, and *black symbols* show cold neutral material. The differences show the importance of measuring all the phases (plasma, gas, and dust) of the interstellar medium



dust within the cloud, which in turn has consequences for the nature of turbulent mixing in the LISM. Moreover, as carbon is a direct pre-requisite for life as we know it, this intriguing puzzle deserves more attention. Direct measurements of singly-ionized and the small expected amount of doubly-ionized Carbon, as well as the dust composition, will shed light on the life-cycle of carbon in the Milky Way.

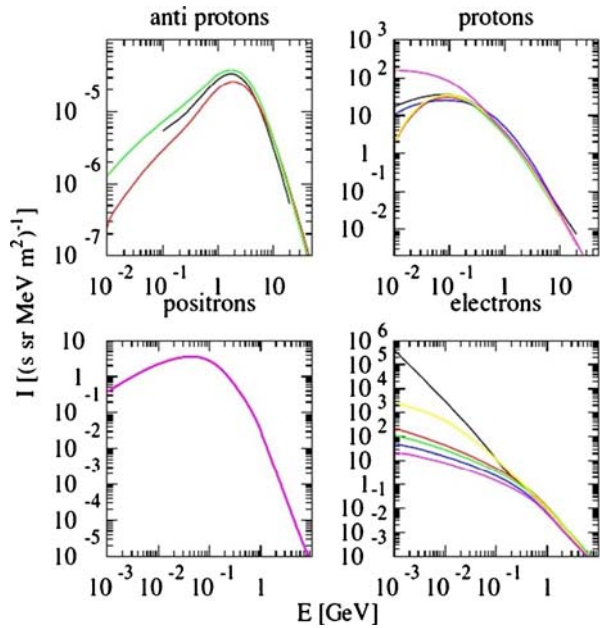
2.3.3 A3: What is the interstellar spectrum of the GCR beyond the heliopause?

The GCR is believed to originate in particles accelerated at supernova-driven shock fronts. These shocks likely accelerate surrounding material, dust, gas, and plasma particles. Thus, GCRs offer a unique way to sample the composition of the galaxy and to understand the energetics of supernova shock expansion. Current modeling efforts show large variations in the possible interstellar spectrum (Fig. 15). One of the difficulties in these studies is the influence of the heliosphere which modifies the GCR spectrum as measured at the Earth. Tremendous gains in the understanding of the above topics could be made if we knew the undisturbed interstellar spectrum. This would allow us to understand and accurately model the filtering effect of the heliosphere and, hence, to much more accurately interpret the information brought to us by galactic cosmic rays. IHP will be able to address this question by measuring the unfolding of the GCR spectrum up to 100–300 MeV/nuc between the outer heliosphere and out beyond the heliopause.

2.3.4 A4: What are the properties of the interstellar magnetic field?

Observations with SOHO/SWAN [32] as well as Voyager radio observations [42] indicate that the magnetic field (likely frozen into the interstellar medium as it also is in the solar wind) does not lie in the galactic plane as would be expected on large scales, but is distorted by the turbulence

Fig. 15 Computed local interstellar spectra of protons and electrons [23]



present in the LIC (Figs. 9 and 16). The direction, strength, and variability of the interstellar magnetic field are key to understanding the overall asymmetric structure of the heliosphere. Current modeling efforts are severely limited by the uncertain knowledge of the interstellar magnetic field and its influence on the heliosphere, a magnetized astrosphere immersed in a turbulent magnetized interstellar environment. The magnetic field strongly influences the flow of charged particles (and, through charge exchange, of neutral particles) and anisotropies of energetic particles and does so on time scales given by the level of interstellar turbulence. The latter is important for the propagation of galactic cosmic rays and for the properties of a number of astrophysical objects. Part of the variability may also be explained by reconnection of the heliospheric and interstellar magnetic field, a fundamental process in astrophysics. Thus, understanding and modeling of the heliosphere, its shielding effects, etc. remain severely limited because the strength of the local interstellar magnetic field is unknown.

2.3.5 A5: What are the properties and dynamics of the interstellar neutral component?

There is overwhelming evidence from the analysis of interstellar absorption lines for the existence of a hydrogen wall (see Figs. 1, 4, and 5 ahead of the heliosphere [20, 33, 57]). Such structures have been observed around other stars [25, 57] as have been bow shocks [4], indicating that our heliosphere is not unique but rather a typical example of an astrosphere forming around

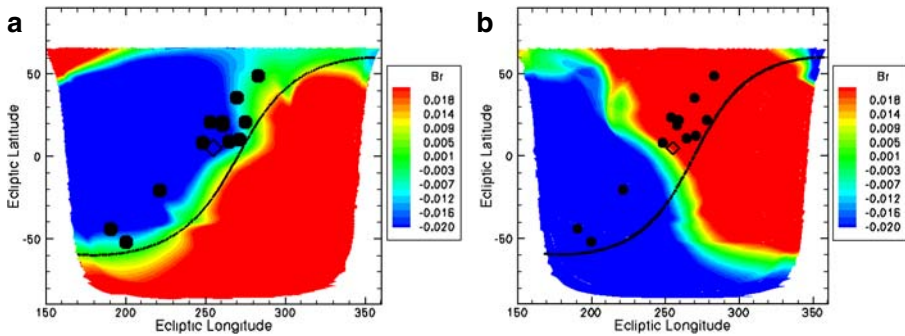


Fig. 16 Radio source location as a function of the interstellar magnetic field (BISM) direction in **a** the plane perpendicular to the radio source plane (with $\alpha = 30^\circ$) and **b** the galactic plane (with $\alpha = 45^\circ$). The direction of the nose of the heliosphere (*diamond*) and the galactic plane (*black line*) are indicated for reference. The radio sources detected by V1 and V2 are shown as *solid circles*. Note that the colors are inverted from **a** to **b** because the interstellar magnetic direction was inverted

each wind-driving star. However, we do not know the properties of the neutral component beyond the heliopause, yet alone understand sufficiently its dynamics in the hydrogen wall and interstellar medium.

The Voyager spacecraft provide some direct information on the plasma environment in the outer heliosphere, but the state of the neutral gas is unknown, and no observations will be available beyond 130–140 AU, where the power supply onboard the Voyagers will become insufficient. Ulysses has measured neutral interstellar gas directly out to ~ 5 AU, and first observations of energetic neutral atoms (ENAs) are confirming their likely production in the (inner) heliosheath between the solar wind termination shock and the heliopause [19, 58]. These pioneering measurements will be routinely performed by the Interstellar Boundary Explorer (IBEX, see [36]) which will map the heliosheath between the termination shock and the heliopause by remote imaging of energetic neutral atoms (ENAs). On the other hand, IBEX will not provide us with measurements beyond this region, especially within the hydrogen wall. These will be performed by IHP/HEX, thus providing us with a detailed understanding of the interstellar neutral component.

2.3.6 A6: What are the properties and dynamics of interstellar dust?

Understanding the nature of the interstellar medium and its interaction with the solar system includes the dust properties in the outer solar system and in the interstellar medium. Moreover improving our knowledge of interstellar dust properties and quantifying the dust to gas ratio in the interstellar medium is of fundamental astrophysical interest. The Ulysses data allowed constraining models of the local interstellar medium physics as well as of interstellar dust [17]. The measurements within the solar system provide valuable information, but they improve our understanding of the interstellar dust only within certain

limits and important parameters like the size distribution of interstellar dust and the dust-to-gas mass ratio can not be measured within the solar system (See A2).

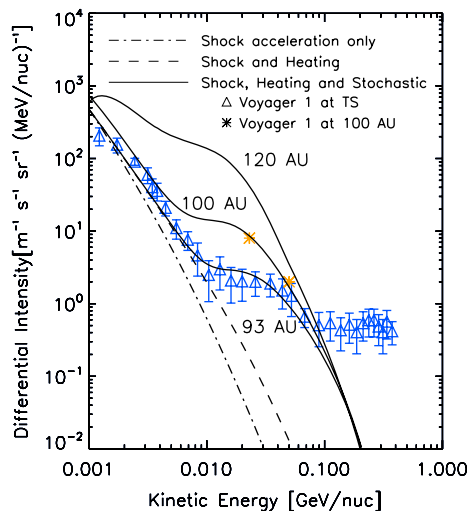
2.4 F: How do plasma, neutral gas, dust, waves, particles, fields, and radiation interact in extremely rarefied, turbulent, and incompletely ionized plasmas?

Our understanding of the physics of complex interstellar plasmas is extremely limited. At least part of the problem lies in the multiple components constituting the interstellar medium which all contribute similarly to, e.g., the pressure in the LISM and the heliospheric boundary region.

2.4.1 F1: What is the nature of wave–particle interaction in the extremely rarefied heliospheric plasma?

As discussed in Section 2.2.4 (H4), the pre-acceleration of the anomalous component is incompletely understood. Why do ACR not peak at the termination shock? Obviously, the magnetic structure in this interface region plays a major role, as does the detailed wave–particle interaction in this turbulent region. While the spectra at higher energies can be modeled fairly accurately with a combination of first-order diffusive (shock) acceleration and second-order (stochastic) Fermi acceleration (Fig. 17), together with limited adiabatic heating, the injection problem at lower energies still remains unsolved. Here, detailed measurements of magnetic field variations and distribution functions of suprathermal particles are key to understanding this problem which, of

Fig. 17 Differential intensity of cosmic ray helium as measured by Voyager 1. From [11]



course, is not limited to particle injection and acceleration in the heliosphere, but must occur at all astrophysical shocks. Thus, it is a prominent example of energy gain by wave–particle interaction (Fig. 10).

2.4.2 F2: How do the multiple components contribute to the definition of the local plasma properties within the heliospheric boundary regions?

Several contributors are about equally important contributors to the pressure in the interstellar medium. GCR pressure, thermal pressure, pickup-ion pressure, magnetic pressure, etc. How can this be treated? Is this a unique situation which allows us to study a kind of plasma that is otherwise not accessible?

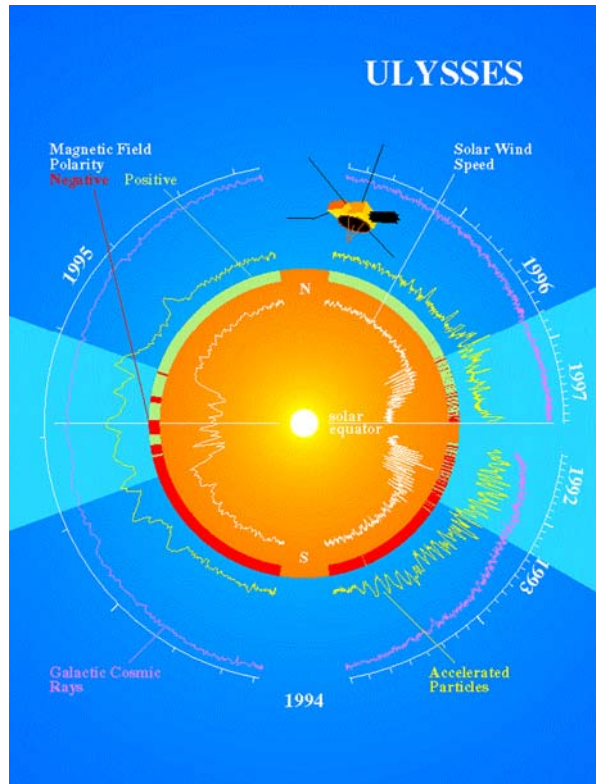
2.4.3 F3: What processes determine the transport of charged energetic particles across a turbulent magnetic field?

Impulsive solar particle events have long been observed at longitudes which appeared to be badly magnetically connected, indicating perpendicular transport, implying action of coronal shocks, or a considerably more complicated magnetic configuration than generally assumed. Similarly, observations of recurrent energetic particle enhancements at much higher latitudes than the accelerating corotating interaction regions (CIRs) appear to imply perpendicular transport or a more complicated heliospheric magnetic configuration that connects CIRs to high latitudes (see Fig. 18 and, e.g., [13], and references therein). Similarly, again, detailed observations of low-energy particle distribution functions in CIRs near Earth were best explained by substantially enhanced transport of particles perpendicular to the magnetic field [10]. Intriguingly, similar phenomena have proved to be extremely puzzling in the fusion community.

2.5 B: What is the cause of the pioneer anomaly?

The first spacecraft to reach the outer heliosphere, Pioneer, had the unique feature of being an extremely simple spacecraft that could be modeled to a high fidelity. Radio tracking of Pioneer revealed a puzzling drift against the expected trajectory which could not be accounted for [1]. Possible fuel tank leakage, light pressure, etc. were considered and rejected as the cause so that today, there is a group of serious scientists who consider this trajectory anomaly as a topic worth serious consideration, even worth a mission within the Cosmic Vision 2015–2025 programme. If confirmed the Pioneer Anomaly would imply the necessity to modify the law of gravitation from Newtonian to a Yukawa-type law. This would be of fundamental significance to astrophysics, cosmology, and our understanding of “how the world is made”. While we do not believe that a dedicated Pioneer-anomaly mission should be flown—no similar anomalies have been seen with other spacecraft, we herewith offer the opportunity to study this anomaly by closely observing IHP/HEX’s trajectory.

Fig. 18 Observations of energetic particles along the Ulysses trajectory showed unexpected recurrent corotating enhancements at high heliographic latitudes



As is discussed in Section 5, the large distance between IHP/HEX and Earth will require use of an ultra-stable oscillator (USO) which will allow extremely precise tracking of the spacecraft trajectory.

3 Mission profile

3.1 Launcher requirements

IHP/HEX currently baselines the use of solar sailing technology to reach the outer solar system in 25 years. The spacecraft itself is very light, the sail structure module as well. Launch mass is on the order of 500–550 kg, required to reach Earth escape orbit. This is a modest requirement and allows us to use a modest launch vehicle. Previous studies ([29], and references therein) have shown that a Soyuz-Fregat delivers sufficient launch capability for IHP/HEX. Nevertheless, as we are baselining the use of US-supplied RPSs, the launcher will likely need to be supplied by NASA as well—we will study the use of Delta IV 4040-12 “Med Lite” and Atlas V 401 during assessment phase.

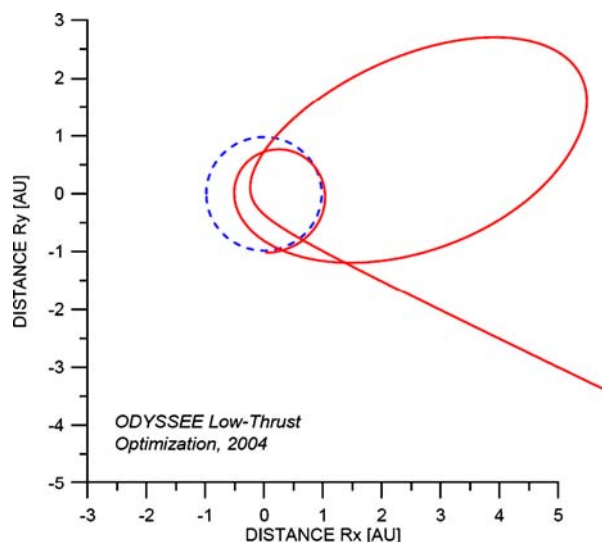
3.2 Orbit requirements

It can be shown that an initial positive hyperbolic excess velocity, $C3$, does not significantly reduce the interplanetary transfer time out to 200 AU and consequently, all calculations presented here have assumed an insertion into interplanetary orbit with essentially zero excess hyperbolic escape velocity and optimization of the orbit was performed from there. Nevertheless, orbit and mission duration optimization with a finite $C3$ is possible, but has not yet been studied by us.

Since the solar radiation pressure declines as $1/r^2$ with distance from the Sun, the propulsive capabilities of a solar sail are more and more limited as proceeding into the outer regions of the solar system. Consequently, continuous outward spiraling to reach the outer solar system is not practicable. However, a sailcraft may gain an enormous amount of orbital energy when first approaching the Sun before proceeding to the outer solar system. By performing such a ‘Solar Photonic Assist’ the transfer orbit about the Sun can turn hyperbolic, allowing reasonable trip times to the outer planets and targets beyond without applying gravity assists. The trajectory design foresees an extended time in the inner solar system prior to reaching hyperbolic energy after the second solar photonic assist. This time spent in the inner solar system which can reach 4 to 7 years is balanced by the higher escape speed which can be achieved by this strategy.

The trajectory shown in Fig. 19 is optimized for minimum flight time to 200 AU. Here, the sailcraft remains within the ecliptic plane as any changes in heliocentric inclination will consume part of the Δv which the sail can generate, thus reducing the escape velocity. Nevertheless, the Δv required to

Fig. 19 Solar sailing cruise orbit. First aphelion at 1.05 AU is reached after about 150 days, first perihelion at 0.51 AU after ~220 days, second aphelion at 5.76 AU after 3.8 years, second perihelion at 0.25 AU after 6.6 years. Sail is jettisoned after 6.7 years, after which the full science mission begins



reach the heliographic equatorial plane inclined at approximately 7° relative to the ecliptic, is small. With the heliocentric escape velocity for this trajectory it is possible to reach 200 AU in a flight time of about 25 years. The transfer time can be reduced by improving the overall mass-to-area ratio, thus increasing the sailcraft acceleration. Here, an acceleration of 1 mm/s^2 at 1 AU was used. This value is based on a $2 \text{ }\mu\text{m}$ polyimide foil (see Section 5). Such foils are currently available on roll widths of 1.5–2 m and improvements towards a $1 \text{ }\mu\text{m}$ foils in sufficiently large size to assemble a sail are highly probable. Having a second perihelion passage enhances the overall mission robustness because it allows to perform orbit corrections after the initial perihelion passage.

The solar sail transfer outlined above does not require a planetary gravity assist to reach solar system escape velocity. It can be shown ([30], and references therein) that the effect of including a Jupiter Gravity Assist (JGA) on the outbound leg is of limited value, and will not significantly contribute to the cruise speed. This is a consequence of the already high cruise speed after the second solar photonic assist. Nevertheless, a Jupiter gravity assist may be helpful to reduce travel time during the first perihelion passage phase.

The cruise phase lasts until sail jettisoning (after 6.7 years in the orbit presented here) and will be used for limited science, especially for the high energy measurements which are not unduly influenced by the large solar sail in the vicinity and possible charging effects. After sail jettisoning, IHP will have a velocity of about 10–11 AU per year and will travel to 200 AU within 20 years.

To summarize, initial studies ([30], and references therein) have demonstrated that IHP/HEX can reach 200 AU in approximately 25 years using solar sail technology only. Trade studies are likely to improve mission robustness and shorten total mission duration or allow us to lower subsystem requirements, or even to reach larger distances from the Sun.

4 Payload

4.1 Overview of all proposed payload elements

In order to achieve the scientific objectives of the IHP, the payload instruments include a magnetometer, plasma analyzer and plasma wave experiment, energetic particle detector, and neutral atom detector. The key resource requirements and characteristics of the instrument are summarized in Table 2.

4.2 Summary of each instruments key resource characteristics

4.2.1 Magnetometer

The magnetic field is a key parameter in any plasma and is central to the science goals of IHP/HEX, as discussed in Section 3. Energetic particle acceleration and transport is controlled by the fluctuating magnetic field. The field plays a key role in shocks, waves and other dynamic phenomena.

Table 2 IHP science payload summary table

Acronym	Instrument	Mass [kg]	Power [W]	Telemetry bps	Volume	Measurements
MAG	Magnetometer	1.5	1.0	50	500	1 Hz magnetic field vectors
PA	Plasma analyzer	2	1.3	30	$25 \times 25 \times 25$	Solar wind and interstellar plasma composition
SWPI	Solar wind inst.	1.5	1.2	30	$25 \times 25 \times 25$	Ions 0.2–50 keV/q
IPS	Interst. plasma	5.8	2.8	30	$19 \times 18 \times 2$	Ions 0.02–20 keV/q
PW	Plasma waves	1.1	1.0	20	plus electronics $24 \times 24 \times 29$	Radio and plasma waves from 10 Hz to 10 MHz
HDA	Dust analyzer	3.0	3.0	10	$15 \times 15 \times 20$	Dust particle velocity and composition
EPD	Energetic particle detector	1.5	2.0	10	$10 \times 10 \times 15$	Particle spectra
STI	Energetic particle detector	3.5	4.0	15	$15 \times 20 \times 25$	He–Fe: 5 keV/n–5 MeV/n charge state; 10–500 keV/q
ELZI	Energetic particle detector	4.5	6.0	20	$60 \times 60 \times 15$ (envelope)	Electrons: 50 keV–2 MeV H and He; 0.1–10 MeV/n
AGCR	Energetic particle detector	1.2	1.5	50	tbd	Electrons: 1–15 MeV H and He; 3–300 MeV/n O–Fe: 5–300 MeV/n
ENI	Energetic neutral imager	25.6	23.8	265	–	Hydrogen ENAs 0.05–4 keV, Ly- α broadband photometry
Ly- α	Ly- α photometer					
Total						

Note that telemetry numbers do not need to be consistent with telemetry rate as not all instruments operate continuously

Topological boundaries, particularly the heliopause, are delineated by the magnetic field. It is therefore essential to measure the local magnetic field with high precision. However, magnetic fields in the outer heliosphere, heliosheath and interstellar medium are extremely low, sometimes around 0.05 nT in magnitude, and present a challenge to any instrument.

The MAG instrument will use tri-axial fluxgate sensors, of conventional design, to measure the magnetic field local to the spacecraft with an accuracy of 0.01 nT. A dual core sensor design, as recently flown on Double Star, provides measurements of all three components of the magnetic field, with a combined sensor and electronics noise level of less than 10 pT at 1 Hz.

The twin MAG sensors will be located on a boom to reduce the effects of stray spacecraft fields. Two sensors dramatically increase the accuracy to which stray fields can be quantified and removed, a key issue with IHP/HEX.

The requirement to measure the ambient field vector with an accuracy of 10% places a strong constraint on MAG: this corresponds to a component precision of around 0.025 nT. This can be achieved with the lowest noise fluxgate sensors currently flown, such as those of Imperial College's industrial partner, Ultra Electronics Ltd, and those flown on Double Star.

4.2.2 Plasma analyzer

The plasma and composition experiment requires a wide viewing geometry and a large dynamic range of sensitivities addressing all key objectives. This instrument will fall into two sensor-heads. The solar wind and pickup ion (SWPI) sensor measures heliospheric plasma, while the interstellar plasma sensor (IPS) determines interstellar plasma composition. Two sensors are needed due to the mutually exclusive field-of-view requirements for the mission phases inside and outside the termination shock. Due to the mission focus on the outer heliosphere both sensors are composed of an electrostatic deflection measurement (E/q filter) with angular resolution and a time-of-flight measurement. Both utilize spacecraft spin for additional direction information.

The SWPI electrostatic design is composed of an E/q deflection system with sweeping voltages for sufficient field-of-view coverage of a 60° cone from the solar direction. The energy-per-charge range should be from 200 eV/e to 50 keV/e. It is also possible to use a fisheye-type electrostatic design, such as used on MESSENGER, or to use a top-hat design. Such designs routinely deflect ions up to 100 keV/e. The time-of-flight section uses a post-acceleration and a thin carbon foil for start measurements, and direct MCP measurements for particle stops. The time-of-flight analysis should preferably use integrated circuits to reduce power and mass needs of the sensor. All electronics parts should be sufficiently radiation hard to manage the life-time dose expected during this mission.

The IPS sensor requires a field-of-view of 45° about the anti-solar direction with an electrostatic design comparable to the SWPI. The energy range should be from 20 eV to 20 keV, with a time-of-flight technique identical to the SWPI. The mass-range should include all components of the interstellar medium and,

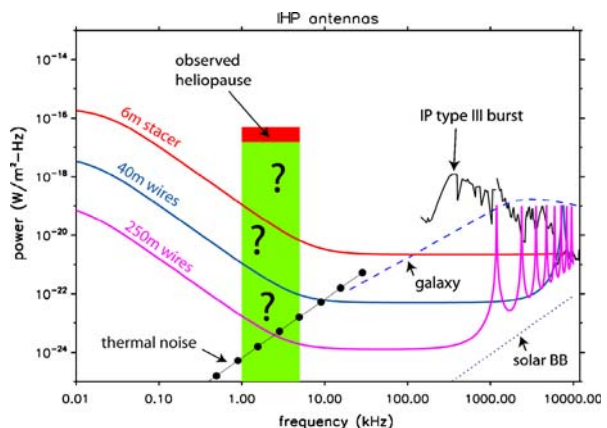
hence, extend to mass ≈ 60 amu. The reduced background requirements due to the anti-solar mounting, and the smaller energy range will allow for a more open design of this instruments with a better ratio of sensitive area to total instrument geometry.

The SWPI and IPS run in two operational modes determined mostly by their time-resolution. SWPI has its primary observations within the heliopause, but remains active beyond that. IPS has its primary observations beyond the heliopause but goes through checkup in the heliosheath. The regular mode to be used in the vast majority of cases provides a steady measurement every 15 min. Higher time-resolution burst data at 1 min resolution are required in the vicinity of large-scale boundaries, such as the termination shock, the heliopause or other dynamic structures.

4.2.3 Plasma waves

The radio and plasma waves (RPW) instrument measures in situ wave fields and remote radio emission on deployable wire electric antennas and a single magnetic loop antenna. Radio emission from near the termination shock is a primary remote diagnostic of shock location and orientation (e.g. [21]) and electron beam-driven Langmuir waves indicate foreshock regions [12, 31]. The RPW instrument will measure these phenomena and do direction-finding measurements on the remote radio emissions. Furthermore, wire antennas can be used to measure dust impacts to the spacecraft; RPW will therefore contribute to the dust objectives. This instrument can have several orders of magnitude more sensitivity than the Voyager instrument (see Fig. 20), by using long wire antennas, a sensitive digital receiver, and having a good EMC program on the spacecraft.

Fig. 20 The radio and plasma waves experiment is a derivative of the Wind and STEREO instruments



4.2.4 Heliopause dust analyzer (HDA)

The dust analyzer measures micrometeoroid impacts to determine their speed, mass and composition using a time-of-flight mass spectrometer based on the design of the Cassini dust detector [54]. This design ensures a high sensitivity (0.1 μm grains at 20 km/s impact speed, a large sensitive area (450 cm^2) to account for the low dust fluxes, a high reliability (coincidence of four impact signals) and the capability to analyze the dust particle composition which is of highest interest for grains in the outer solar system (mass resolution ~ 50). This spectrometer type showed excellent performance in the Saturnian system on the Cassini probe [44] and reliably distinguishes icy particles from silicates, carbon-rich and metallic particles. In contrast to the dust detector onboard New Horizon this instrument has a ten times higher sensitivity, a higher reliability and provides the dust composition. The detector consists of a hemispherical rhodium plated target with a diameter of 240 mm. Hypervelocity impacts of micrograins generate an impact plasma above the target. The impact plasma is separated in an electric field of 2,000 V/cm by an acceleration grid which is located 1 cm in front of the target. The negative electrons are collected by the target and a charge sensitive amplifier (CSA) measures the charge and triggers the data acquisition. The instrument contains three grids: Two large grids in front of the target (acceleration grid and shielding grid) and a small ion grid at the aperture of central ion collector (multi-channel plate). The ions are accelerated towards the central ion collector mounted 223 mm above the target. CSAs at the acceleration grid and the ion grid provide a positive ion signal in conjunction with the mass spectrum at the ion collector. The ion collector provides the mass spectrum and uses a 100 MHz analog-to-digital conversion. A target heating (5 W) decontaminates the target twice a year and a fly-away cover avoids contaminations before launch. The electronics uses FPGA and ASIC technology and is housed below the target (Fig. 21).

4.2.5 Energetic particle detector

Measurements of energetic particles are essential for three of the five main scientific goals of the IHP. The observations have to cover a wide range of species from electrons and protons to iron group of elements and from suprathermal energies to galactic cosmic rays. To achieve this, the energetic particle detector consists of three units operating in various energy ranges.

The SupraThermal Ion spectrometer (STI) measures ions from helium to iron in the energy range 5keV/n to 5MeV/n. The charge states of heavy ions are determined in the more limited range of 10–500 keV/q. STI employs both an electrostatic analyzer and time-of-flight method together with energy measurement.

Electrons between 50 keV and 2 MeV and protons and helium nuclei in the range 0.1–10 MeV/n are measured by the Electron and Low-Z Ion telescope (ELZI). ELZI relies on conventional silicon technology with energy loss-residual energy (dE-E) measurements to identify the incident particles.

Fig. 21 The Heliopause Dust Sensor is a derivative of the very successful Cassini dust sensor



Measurements at highest energies are carried out by the Anomalous and Galactic Cosmic Ray telescope (AGCR) employing the dE-E and range technique. This instrument is a double-ended telescope with electrons (1–15 MeV) and high-energy protons (3–300 MeV) measured from one direction and ions from helium to iron up to 300 MeV/n from the opposite end. The purpose of this arrangement is to limit the required dynamic range of the electronics to reasonable values.

4.2.6 Energetic neutral imager

The ENA sensor consists of nine individual sensors (directional channels) in the fan configuration. Each channel has $20^\circ \times 20^\circ$ field of view. The bore-sight lines are in the spacecraft spin axis plane. Therefore, for each spin the instrument covers the full 2π and produces a single image. In each telescope the incoming charged particles are removed by an electrostatic deflector. ENAs hit a conversion surface and converted to negative ions, which are transported by an energy dispersive ion optics to a position sensitive MCP detector. The position of the signal gives the ENA energy. The ion channel is complemented by a neutral channel of higher sensitivity for energies >0.2 keV. It operates on large distances from the Sun when the UV background sufficiently reduced. In this channel ENAs impacting the surface produce kinetic secondary electrons, which are used to generate START pulse for time-of-flight electronics, and then hit STOP detector generating STOP pulse. This coincidence scheme also allows higher signal-to-noise ratio. This channel is also required for inter calibrations against a stellar UV source. The architecture with nine sensors is required to solve the problem of the full angular coverage from a spacecraft with a spin axis fixed in the inertial frame. In principle, a combination of a

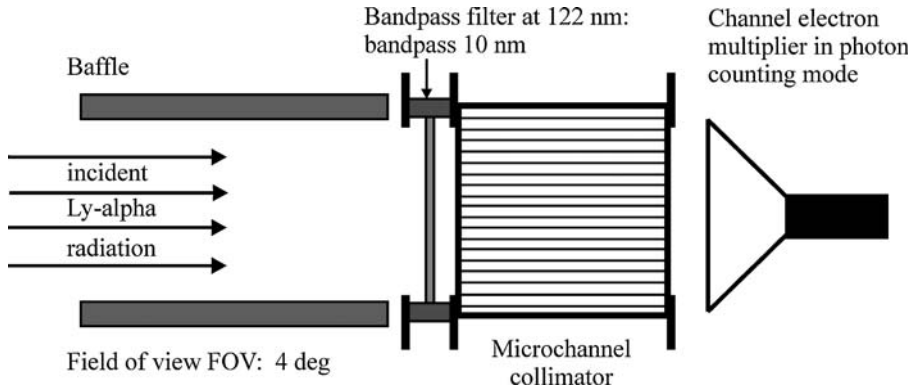


Fig. 22 UV photometer

single sensor and a mechanical scanner can also provide the required coverage but keeping in mind the required long life time of the mission this approach is less favorable.

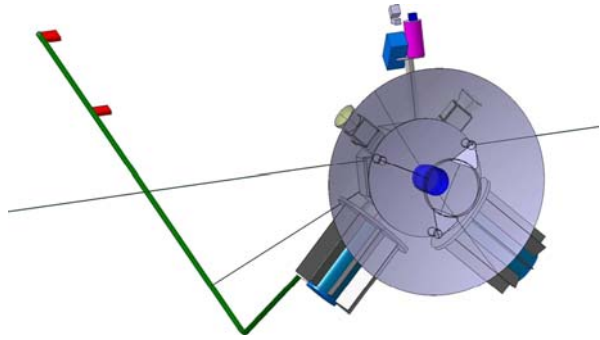
4.2.7 Ly- α experiment

Three miniature broadband Ly- α photometers will measure the intensity of solar Ly- α resonantly backscattered by atomic hydrogen (Fig. 22). Each photometer has a FOV of $\sim 4^\circ \times 4^\circ$ and a sensitivity between 1.8 and 2.2 photon counts per second per Rayleigh. We expect a brightness of 20 R at 100 AU, 10 R at 200 AU, and 7 R at 300 AU. Thus, a determination of line-of-sight neutral hydrogen column density in a $\sim 4^\circ \times 4^\circ$ FOV to within one percent will require less than 20 min operation. The 4° FOV along the spin direction (perpendicular to the spin axis) fit in 90 times, thus, the Ly- α photometer will not be operated in a continuous mode, but approximately 1 day every month, i.e., about once for every AU progress along the trajectory. These observations along IHP's trajectory will allow us to tomographically reconstruct the three-dimensional structure of the hydrogen wall and neutral hydrogen density throughout the heliosphere, while long-term observations will allow us to determine the galactic Ly- α background. The instrument is calibrated in flight using the known Ly- α intensity of a number of reference stars.

5 Spacecraft

IHP/HEX will require one spacecraft defined further down (Fig. 23). Should there be a request to combine IHP/HEX with one of the proposals to study the Pioneer Anomaly, a test mass may be necessary. Note that this is not needed for the core IHP/HEX science objectives, we do not request this.

Fig. 23 Science configuration of the IHP spacecraft



5.1 Spacecraft architecture

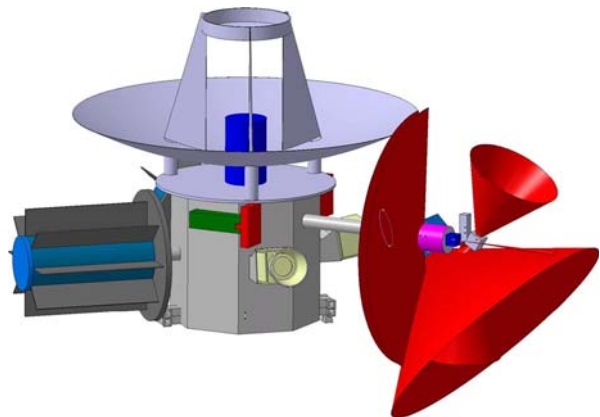
The design of the spacecraft in the solar sail configuration, also referred to as the sailcraft, is shown in the following figures. In general, according to the baseline mission where the sail is jettisoned at 5 AU solar distance, after achieving solar system escape energy, the following main operation modes are distinguished:

- Sailing mode with the sail attached, and where the sail is required to perform an optimal sail maneuvering during the cruise phase in the inner solar system,
- Science mode, which starts at 5 AU, after sail jettisoning.

Consequently, two principal spacecraft configurations were defined: the sailing mode in which the solar sail structure is attached, and the science mode after the sail has been jettisoned (Fig. 24).

Figure 25 shows the spacecraft with launch adapter and in the sailing mode with solar sail deployed. The platform is offset from the sail area via a deployable Sailcraft Control Mast. Together with a two Degree of Freedom

Fig. 24 Payload elements with FOVs



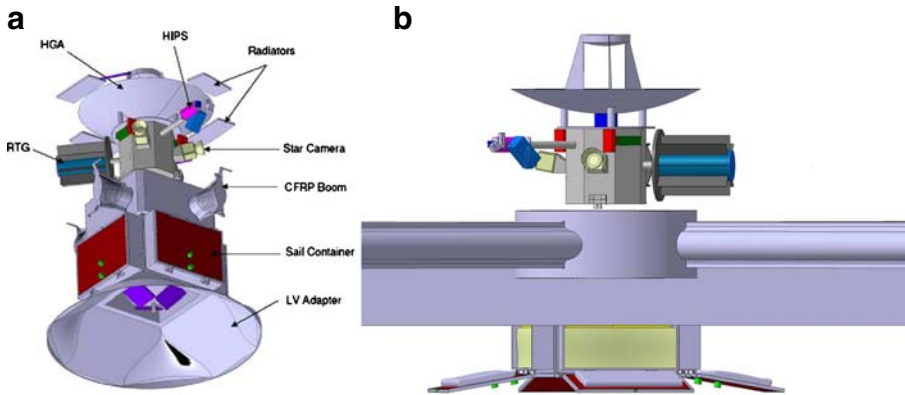
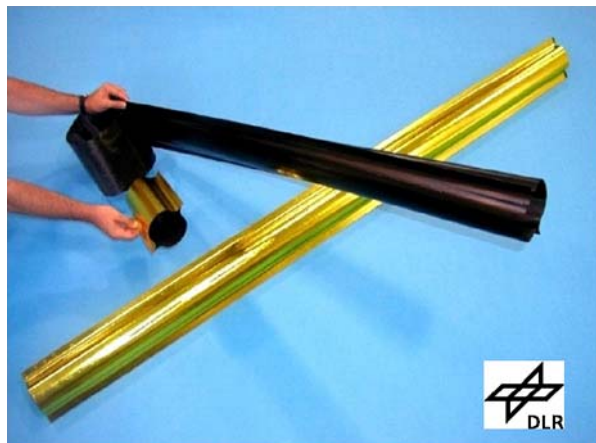


Fig. 25 a Stowed configuration with launch adapter. b Spacecraft with solar sail deployed

(DOF) gimbal joint at the center of the sail structure this will allow to introduce an offset of the center-of-mass (COM) to the center-of-pressure (COP) and the generation of an external torque due to solar pressure for sailcraft attitude control.

The sail structure is composed of three major elements, the deployable booms, a central Deployment Module, and the sail film segments. The four supporting CFRP booms are unrolled from the central Deployment Module, and the four folded, triangular sail film segments are released from sail containers which are part of the central Deployment Module. The deployable booms, developed by the DLR Institute of Structural Mechanics, combine high strength and stiffness with extremely low density and can be stored within a very tight volume. The booms consist of two question-mark-shaped (?-shaped) laminated shells which are bonded at the edges to form a tubular shape. They

Fig. 26 Solar sail CFRP booms



can be pressed flat around a central hub for storage, and uncoil from the central hub during deployment (Fig. 26).

Once free of the Deployment Module, the booms resume their original tubular shape with high bending stiffness. The concept has successfully been demonstrated in a ground test campaign. In stowed configuration all four booms are co-coiled on a central hub. A mechanism allows to simultaneously deploying all booms in a controllable way. Besides the compartment housing the coiled booms and the associated deployment mechanisms the Deployment Module has four individual sail containers which house the folded sails for the launch phase prior to deployment in space. The baseline for the sail material is a thin (1–2 μm thick) Polyimide film coated on the front side with Aluminium and a back-side Cr coating.

ESA has already conducted a technology reference study for IHP/HEX. More details on spacecraft design can be found in [28].

5.2 Estimated overall resources (mass and power)

The mission places a high demand on the power subsystem which needs to supply the spacecraft with on-board power of a solar range of 0.25 to 200 AU. First analyses in power consumption have shown that the power subsystem requirements are 120 avg./145 W peak (EOL min) and 150/190 W (Design/BOL). BOL peak power requirements are entirely driven by the deployment of the solar sails. Following previous trade-offs with other propulsion/power systems, RPSs are the most promising option as they also have the necessary flight heritage. However using RPSs is a very sensitive and challenging issue due to limited availability, long lead times and political issues related to RPS purchase. Specific power (W/kg) is the key factor in RPSs. The key assumption in designing the power subsystem is the 8 W/kg specific power figure (2nd generation RPS) and a degradation rate of 1 W/year. Thermal power must be radiated, hence the large fins and the heat shield between the RPS and the spacecraft. The Multi-Mission RPS (MMRTG) under development for Prometheus is based on the GPHS module, with a desired power output

Table 3 Estimated mass and power resources

Item	Mass w/o margin (kg)	Mass w margin (kg)	Power average (W)	Power peak (W)
Platform w/o payload	138	170	67	75
Solar sail assembly	175	205	40	65
S/C adaptor	36	45		
Payload	17	21	35	40
Launch mass	366	431		
System-level margin		86	20	20
Launch with margin		517	160 (BOL)	190 (BOL)

Power numbers do not need to add up, as not all elements are used at the same time. The last line gives available power at beginning of life (BOL). Total available power includes 20% margin and DC/DC conversion efficiency

of 100 W estimated from a wide ranging mission analysis. The goal of the MMRTG program is to provide sufficient power for many missions while reducing the carried Plutonium. For the heliopause mission two RPSs will be required, placed opposite to the highly integrated payload suite (Table 3). More details on the resource allocation can be found in [27].

6 Summary and conclusions

The heliosphere is the only astrosphere which we can investigate in any meaningful detail, in situ, and for which we have long-term archives in the form of asteroidal and lunar regoliths. While substantial improvements in our understanding of the structure and dynamics of the heliosphere have been made thanks to spacecraft launched by ESA and NASA, the next logical step to complete the missing link is to investigate in-situ the boundary layers of the heliosphere, terminations shock, heliopause, and, eventually, the bow shock. To this end we have proposed the Interstellar Heliopause Probe/Heliospheric Boundary Explorer (IHP/HEX) in a truly international effort involving scientists from 17 countries. IHP/HEX will reach the heliopause within the career of a scientist using solar sailing technology, thus also driving and opening a new era of space transportation.

IHP/HEX is highly relevant to the four Science Themes defined for the Cosmic Vision 2015–2025 programme and addresses all of them:

CV-2015–2025 theme	IHP/HEX relevance
What are the conditions for planet formation and the emergence of life?	Shielding of GCR, dust, and neutrals; dust–plasma interactions
How does the solar system work?	Heliospheric science focus
What are the fundamental physical laws of the universe?	Fundamental plasma physics; extremely rarefied plasmas
How did the universe originate and what is it made of?	LISM composition and galactic chemical evolution

Carrying through a successful IHP/HEX mission will require development efforts in technology but also careful science policy to ensure that the required scientific and technological knowledge will survive over the course of the mission. On the technology development side, the foremost drivers will be solar sailing, light-weight but high-power RPSs, and communications. All three developments would greatly enhance the accessibility of potential science targets such as high-inclination heliospheric orbits, exploration of distant objects, but also establishing a long-term presence in locations which make solar power inefficient due to distance from the Sun or permanent shadow or dense cloud cover. Thus, IHP/HEX serves as a “condensation nucleus” for developing technologies which are key also to other science missions in the solar system.

The first steps that need to be taken are a technology-demonstrator mission, such as ESA’s Geosail technology reference study which would demonstrate

key solar sailing properties, such as manoeuvrability, attitude control, thrust, ageing properties, surface charging, etc.

The IHP/HEX team

IHP/HEX was proposed by the following large international team:

- Germany: H. Fahr, hfahr@astro.uni-bonn.de, H. Fichtner, hf@tp4.ruhr-uni-bochum.de, B. Heber, heber@physik.uni-kiel.de, U. Mall, mall@linmpi.mpg.de, I. Mann, imann@uni-muenster.de, E. Marsch, marsch@linmpi.mpg.de, K.-H. Glassmeier, kh.glassmeier@tu-bs.de, H. Kunow, kunow@physik.uni-kiel.de, B. Klecker, berndt.klecker@mpe.mpg.de, J. Woch, woch@linmpi.mpg.de, R. Srama, ralf.srama@mpi-hd.mpg.de, K. Scherer, klaus.scherer@dat-hex.de, M. Witte, witte@linmpi.mpg.de, R. F. Wimmer-Schweingruber, wimmer@physik.uni-kiel.de, W. Droege, Wolfgang.Droege@astro.uni-wuerzburg.de, M. Leipold, manfred.leipold@kayser-threde.com, K. Mannheim, mannheim@astro.uni-wuerzburg.de, R. Schlickeiser, rsch@tp4.ruhr-uni-bochum.de,
- Switzerland: P. Wurz, peter.wurz@soho.unibe.ch, P. Bochsler, Bochsler@soho.unibe.ch, R. v. Steiger, rudolf.vonsteiger@issi.unibe.ch, J. Geiss, geiss@issi.unibe.ch
- France: R. Lallement, rosine.lallement@aerov.jussieu.fr, J.-L. Bougeret, jean-louis.bougeret@obsmp.fr, E. Quemerais, eric.quemerais@aerov.jussieu.fr, M. Maksimovic, milan.maksimovic@obsmp.fr, C. Briand, carine.briand@obsmp.fr
- Italy: R. Bruno, roberto.bruno@ifsi.rm.cnr.it, B. Bavassano, bavassano@ifsi.rm.cnr.it, G. Zimbardo, zimbardo@fis.unical.it, M. Velli, velli@arcetri.astro.it, L. Sorriso-Valvo, sorriso@fis.unical.it, M. Casolino, Marco.Casolino@roma2.infn.it,
- Austria: Helmut Rucker, rucker@oeaw.ac.at, D. Breitschwerdt, breitschwerdt@astro.univie.ac.at
- Norway: V. Hansteen, viggoh@astro.uio.no, O. Lie-Svendsen, oystein.lie-svendsen@ffi.no
- Great Britain: T. Horbury, t.horbury@ic.ac.uk, A. Balogh, a.balogh@imperial.ac.uk, R. Forsyth, r.forsyth@ic.ac.uk
- Greece: S. Krimigis, tom.krimigis@jhuapl.edu
- Finland: J. Torsti, Jarmo.Torsti@srl.utu.fi, L. Kocharov, Leon.Kocharov@srl.utu.fi, E. Valtonen, Eino.Valtonen@srl.utu.fi, E. Kyrölä, erkki.kyrola@fmi.fi, P. Janhunen, pekka.janhunen@fmi.fi, T. Laitinen, timo.laitinen@utu.fi, W. Schmidt, Walter.Schmidt@fmi.fi
- Poland: R. Ratkiewicz, roma@cbk.waw.pl, A. Czechowski, ace@telemann.cbk.waw.pl, M. Bzowski, bzowski@cbk.waw.pl
- Sweden: S. Barabash, stas@irf.se
- Russia: V. Izmodenov, izmod@ipmnet.ru, V.B. Baranov, baranov@ipmnet.ru, Y.G. Malama, malama@ipmnet.ru, S. Chalov, chalov@ipmnet.ru, D. Alexashov, alexash@ipmnet.ru, I. Kolesnikov, garikol@inbox.ru, E. Provornikova, provea@mail.ru, Y. Yermolaev, yermol@iki.rssi.ru, M. Panasyuk, panasyuk@sinp.msu.ru
- USA: G. Zank, zank@ucacl.ucr.edu, E. Moebius, Eberhard.Moebius@unh.edu, T. Zurbuchen, thomasz@umich.edu, G. Mason, glenn.mason@jhuapl.edu, M.E. Hill, matt.hill@jhuapl.edu, J. Mazur, Joseph.E.Mazur@aero.org, G. Gloeckler, gglo@umich.edu, R. Mewaldt, mewaldt@srl.caltech.edu, M. Lee, marty.lee@unh.edu, P. Liewer, paulett.liewer@jpl.nasa.gov, R. Lin, rln@ssl.berkeley.edu, S. Bale, bale@ssl.berkeley.edu, D. McComas,

dmccomas@swri.edu, H. Funsten, hfunsten@lanl.gov, N. Schwadron, nathanas@bu.edu, M. Opher, mopher@physics.gmu.edu, F. Allegrini, fallegrini@swri.edu, R. McNutt, ralph.mcnutt@jhuapl.edu, J. Le Roux, leroux@bartol.udel.edu, M. desai, mdesai@swri.edu, aposner@swri.edu, P. Frisch, frisch@oddjob.uchicago.edu, S. Fuselier, stephen.a.fuselier@lmco.com, M. Gruntman, mikeg@usc.edu, K.-H. Trattner, trattner@mail.spasci.com, J. Slavin, jslavin@cfa.harvard.edu

South Africa: A. Burger, adri.burger@nwu.ac.za, M. Potgieter, fskmsp@puknet.puk.ac.za, S. Ferreira, fsksesf@puknet.puk.ac.za

Australia: I. Cairns, cairns@physics.usyd.edu.au

Canada: S. Sreenivasan, srs@phas.ualgary.ca

Taiwan: W. Ip, wingip@astro.ncu.edu.tw

References

- Anderson, J.D., Laing, P.A., Lau, E.L., Liu, A.S., Nieto, M.M., Turyshev, S. G.: Indication, from Pioneer 10/11, Galileo, and Ulysses Data, of an apparent anomalous, weak, long-range acceleration. *Phys. Rev. Lett.* **81**, 2858–2861 (1998)
- Beer, J., Blinov, A., Bonani, G., Finkel, R.C., Hofmann, H.J., Lehmann, B., Oeschger, H., Sigg, A., Schwander, J., Staffelbach, T., et al.: Use of ^{10}Be in polar ice to trace the 11-year cycle of solar activity. *Nature* **347**, 164–166 (1990)
- Breitschwerdt, D., de Avillez, M.A.: The history and future of the Local and Loop I bubbles. *Astron. Astrophys.* **452**, L1–L5 (2006). doi:[10.1051/0004-6361:20064989](https://doi.org/10.1051/0004-6361:20064989)
- Brown, D., Bomans, D.J.: To see or not to see a bow shock. Identifying bow shocks with $\text{H}\alpha$ allsky surveys. *Astron. Astrophys.* **439**, 183–194 (2005)
- Burlaga, L.F., Ness, N.F., Acuña, M.H., Lepping, R.P., Connerney, J.E.P., Stone, E.C., McDonald, F.B.: Crossing the termination shock into the heliosheath: magnetic fields. *Science* **309**, 2027–2029 (2005)
- Burlaga, L.F., Ness, N.F., Belcher, J.W., Szabo, A., Isenberg, P.A., Lee, M.A.: Pickup protons and pressure-balanced structures: Voyager 2 observations in merged interaction regions near 35 AU. *J. Geophys. Res.* **99**, 21511–21524 (1994)
- Burns, J.A., Lamy, P.H., Soter, S.: Radiation forces on small particles in the solar system. *Icarus* **40**, 1–48 (1979)
- Cummings, A.C., Stone, E.C., Steenberg, C.D.: Composition of anomalous cosmic rays and other heliospheric ions. *Astrophys. J.* **578**, 194–210 (2002)
- Czechowski, A., Mann, I.: Penetration of interstellar dust grains into the heliosphere. *J. Geophys. Res. (Space Physics)* **108**, LIS13.1–LIS13.9 (2003)
- Dwyer, J.R., Mason, G.M., Mazur, J.E., Jokipii, J.R., von Rosenvinge, T.T., Lepping, R.P.: Perpendicular transport of low-energy corotating interaction region-associated nuclei. *Astrophys. J.* **490**, L115–L118 (1997)
- Ferreira, S.E.S., Potgieter, M.S., Scherer, K.: Transport and acceleration of anomalous cosmic rays in the inner heliosheath. *J. Geophys. Res. (Space Physics)*. **112**(A11), 11101 (2007). doi:[10.1029/2007JA012477](https://doi.org/10.1029/2007JA012477)
- Filbert, P.C., Kellogg, P.J.: Electrostatic noise at the plasma frequency beyond the earth's bow shock. *J. Geophys. Res.* **84**, 1369–1381 (1979). doi:[10.1029/JA084iA04p01369](https://doi.org/10.1029/JA084iA04p01369)
- Fisk, L.A., Jokipii, J.R.: Mechanisms for latitudinal transport of energetic particles in the Heliosphere. *Space Sci. Rev.* **89**, 115–124 (1999)
- Fisk, L.A., Kozlovsky, B., Ramaty, R.: An interpretation of the observed oxygen and nitrogen enhancements in low-energy cosmic rays. *Astrophys. J.* **190**, L35–L37 (1974)
- Florinski, V., Zank, G.P.: Particle acceleration at a dynamic termination shock. *Geophys. Res. Lett.* **33**, L15110.1–L15110.5 (2006)
- Florinski, V., Zank, G.P., Pogorelov, N.V.: Galactic cosmic ray transport in the global heliosphere. *J. Geophys. Res.* **108**, 1228 (2003)

17. Frisch, P.C., Dorschner, J.M., Geiss, J., Greenberg, J.M., Grün, E., Landgraf, M., Hoppe, P., Jones, A.P., Krättschmer, W., Linde, T. J., et al.: Dust in the local interstellar wind. *Astrophys. J.* **525**, 492–516 (1999)
18. Frisch, P.C., Slavin, J.D.: Short-term variations in the galactic environment of the sun. *ArXiv Astrophysics e-prints*
19. Galli, A., Wurz, P., Barabash, S., Grigoriev, A., Lundin, R., Futaana, Y., Gunell, H., Holmström, M., Roelof, E.C., Curtis, C.C., et al.: Direct measurements of energetic neutral hydrogen in the interplanetary medium. *Astrophys. J.* **644**, 1317–1325 (2006)
20. Gayley, K.G., Zank, G.P., Pauls, H.L., Frisch, P.C., Welty, D.E.: One- versus two-shock heliosphere: constraining models with Goddard high resolution spectrograph Ly alpha spectra toward alpha centauri. *Astrophys. J.* **487**, 259 (1997)
21. Gurnett, D.A., Allendorf, S.C., Kurth, W.S.: Direction-finding measurements of heliospheric 2–3kHz radio emissions. *Geophys. Res. Lett.* **25**, 4433 (1998). doi:[10.1029/1998GL900201](https://doi.org/10.1029/1998GL900201)
22. Grün, E., Srama, R., Krüger, H., Kempf, S., Dikarev, V., Helfert, S., Moragas-Klostermeyer, G.: 2002 Kuiper prize lecture: dust astronomy. *Icarus* **174**, 1–14 (2005)
23. Heber, B., Ferrando, P., Paizis, C., Müller-Mellin, R., Kunow, H., Potgieter, M.S., Ferreira, S.E.S., Burger, R.A.: Latitudinal gradients and charge sign dependent modulation of galactic cosmic rays. In: Scherer, K., Fichtner, H., Fahr, H.J., Marsch, E. (eds.) *The Outer Heliosphere: The Next Frontiers*, p 191 (2001)
24. Ip, W.-H. and Axford, W.I.: Estimates of galactic cosmic ray spectra at low energies. *Astron. Astrophys.* **149**, 7–10 (1985)
25. Izmodenov, V.V., Geiss, J., Lallement, R., Gloeckler, G., Baranov, V.B., Malama, Y.G.: Filtration of interstellar hydrogen in the two-shock heliospheric interface: inferences on the local interstellar cloud electron density. *J. Geophys. Res.* **104**, 4731–4742 (1999)
26. Jokipii, J.R.: The magnetic field structure in the heliosheath. *Astrophys. J.* **631**, L163–L165 (2005)
27. Kayser-Threde: Preliminary resource allocation & propulsion trades. Technical Report IHP-TN-KTH-0001, Kayser-Threde (2004a)
28. Kayser-Threde: Spacecraft design and budgets. Technical Report IHP-TN-KTH-0001, Kayser-Threde (2004b)
29. Kayser-Threde: Interstellar heliopause probe summary report. Technical Report IHP-TN-KTH-0011, Kayser-Threde (2004)
30. Kayser-Threde: Interstellar heliopause probe summary report. Technical Report IHP-TN-KTH-0011, Kayser-Threde (2005)
31. Kurth, W.S., Gurnett, D.A.: Plasma waves as indicators of the termination shock. *J. Geophys. Res.* **98**, 15129 (1993). doi:[10.1029/93JA01176](https://doi.org/10.1029/93JA01176)
32. Lallement, R., Quémerais, E., Bertaux, J.L., Ferron, S., Koutroumpa, D., Pellinen, R.: Deflection of the interstellar neutral hydrogen flow across the heliospheric interface. *Science* **307**, 1447–1449 (2005)
33. Linsky, J.L., Wood, B.E.: The alpha Centauri line of sight: D/H ratio, physical properties of local interstellar gas, and measurement of heated hydrogen (The ‘Hydrogen Wall’) near the heliopause. *Astrophys. J.* **463**, 254 (1996)
34. Mann, I., Czechowski, A., Grzedzielski, S.: Dust measurements at the edge of the solar system. *Adv. Space Res.* **34**, 179–183 (2004)
35. Mazur, J.E., Mason, G.M., Blake, J.B., Klecker, B., Leske, R.A.,Looper, M.D., Mewaldt, R. A.: Anomalous cosmic ray argon and other rare elements at 1 – 4 MeV/nucleon trapped in the Earth’s magnetosphere. *J. Geophys. Res.* **105**, 21015–21023 (2000)
36. McComas, D.J., Allegrini, F., Bartolone, L., Bochsler, P., Bzowski, M., Collier, M., Fahr, H., Fichtner, H., Frisch, P., Funsten, H., et al.: The interstellar boundary explorer (IBEX): update at the end of phase B. In: Heerikhuisen, J., Florinski, V., Zank, G.P., Pogorelov, N.V. (eds.) *Physics of the Inner heliosheath*, vol. 858 of American Institute of Physics Conference Series, pp. 241–250 (2006)
37. McComas, D.J., Schwadron, N.A.: An explanation of the Voyager paradox: particle acceleration at a blunt termination shock. *Geophys. Res. Lett.* **33**, 4102 (2006)
38. McDonald, F.B.: Cosmic-ray modulation in the heliosphere a phenomenological study. *Space Sci. Rev.* **83**, 33–50 (1998). adsabs.harvard.edu/abs/1998SSRv...83...33M. Provided by the SAO/NASA Astrophysics Data System

39. McDonald, F.B., Webber, W.R., Stone, E.C., Cummings, A.C., Heikkila, B.C., Lal, N.: Voyager observations of galactic and anomalous cosmic rays in the heliosheath. In: Heerikhuisen, J., Florinski, V., Zank, G.P., Pogorelov, N.V. (eds.) *Physics of the Inner Heliosheath*, vol. 858 of American Institute of Physics Conference Series, pp. 79–85 (2006)
40. Mewaldt, R.A., Cummings, A.C., Stone, E.C.: Anomalous cosmic rays: Interstellar interlopers in the heliosphere and magnetosphere. *EOS Transactions* **75**, 185 (1994). doi:[10.1029/94EO00864](https://doi.org/10.1029/94EO00864)
41. Möbius, E., Bzowski, M., Müller, H.-R., Wurz, P.: Effects in the inner heliosphere caused by changing conditions in the galactic environment. In: Frisch, P.C. (ed.) *Solar Journey: the Significance of our Galactic Environment for the Heliosphere and Earth*. University of Chicago, IL, USA. *Astrophysics and Space Science Library*, vol. 338. Springer Dordrecht (2006)
42. Opher, M., Stone, E.C., Gombosi, T.I.: The orientation of the local interstellar magnetic field. *Science* **316**, 875–878 (2007)
43. Pesses, M.E., Eichler, D., Jokipii, J.R.: Cosmic ray drift, shock wave acceleration, and the anomalous component of cosmic rays. *Astrophys. J.* **246**, L85–L88 (1981)
44. Postberg, F., Kempf, S., Srama, R., Green, S.F., Hillier, J.K., McBride, N., Grün, E.: Composition of jovian dust stream particles. *Icarus* **183**, 122–134 (2006). doi:[10.1016/j.icarus.2006.02.001](https://doi.org/10.1016/j.icarus.2006.02.001)
45. Raisbeck, G.M., Yiou, F., Bourles, D., Lorius, C., Jouzel, J., Barkov, N.I.: Evidence for two intervals of enhanced ^{10}Be deposition in Antarctic ice during the last glacial period. *Nature* **326**, 273–277 (1987)
46. Reames, D.V.: Quiet-time spectra and abundances of energetic particles during the 1996 solar minimum. *Astrophys. J.* **518**, 473–479 (1999)
47. Scherer, K., Fichtner, H., Borrmann, T., Beer, J., Desorgher, L., Flükiger, E., Fahr, H.-J., Ferreira, S.E.S., Langner, U. W., Potgieter, M.S., et al.: Interstellar–terrestrial relations: variable cosmic environments, the dynamic heliosphere, and their imprints on terrestrial archives and climate. *Space Sci. Rev.* **127**, 327–465 (2006)
48. Scherer, K., Fichtner, H., Stawicki, O.: Shielded by the wind: the influence of the interstellar medium on the environment of the earth. *J. Atmos. Sol. Ter. Phys.* **64**, 795–804 (2002)
49. Schwadron, N.A., Combi, M., Huebner, W., McComas, D.J.: The outer source of pickup ions and anomalous cosmic rays. *Geophys. Res. Lett.* **29**, 54.1–54.4 (2002)
50. Schwadron, N.A., Fisk, L.A., Gloeckler, G.: Statistical acceleration of interstellar pick-up ions in co-rotating interaction regions. *Geophys. Res. Lett.* **23**, 2871–2874 (1996)
51. Slavin, J.D., Frisch, P.C.: Evidence of a high carbon abundance in the local interstellar cloud. *Astrophys. J.* **651**, L37–L40 (2006)
52. Slavin, J.D., Frisch, P.C.: The chemical composition of interstellar matter at the solar location. *Space Sci. Rev.* **130**, 409–414 (2007)
53. Stone, E.C., Cummings, A.C., McDonald, F.B., Heikkila, B.C., Lal, N., Webber, W.R.: Voyager 1 explores the termination shock region and the heliosheath beyond. *Science* **309**, 2017–2020 (2005)
54. Srama, R., Ahrens, T.J., Altobelli, N., Auer, S., Bradley, J.G., Burton, M., Dikarev, V.V., Economou, T., Fechtig, H., Görlich, M., et al.: The cassini cosmic dust analyzer. *Space Sci. Rev.* **114**, 465–518 (2004). doi:[10.1007/s11214-004-1435-z](https://doi.org/10.1007/s11214-004-1435-z)
55. UNSCEAR: United Nations Scientific Committee on the Effects of Atomic Radiation: UNSCEAR 1993 Report to the General Assembly, with Scientific Annexes. United Nations, New York (1993)
56. Witte, M.: Kinetic parameters of interstellar neutral helium. Review of results obtained during one solar cycle with the Ulysses/GAS-instrument. *Astron. Astrophys.* **426**, 835–844 (2004)
57. Wood, B.E., Redfield, S., Linsky, J.L., Müller, H.-R., Zank, G.P.: Stellar Ly α emission lines in the hubble space telescope archive: intrinsic line fluxes and absorption from the heliosphere and astrospheres. *Astrophys. J. Suppl.* **159**, 118–140 (2005)
58. Wurz, P., Galli, A., Barabash, S., Grigoriev, A.: Energetic neutral atoms from the heliosheath. In: Heerikhuisen, J., Florinski, V., Zank, G.P., Pogorelov, N.V. (eds.) *Physics of the inner heliosheath* vol. 858 of American Institute of Physics Conference Series, pp. 269–275 (2006)
59. Yamamoto, S., Mukai, T.: Dust production by impacts of interstellar dust on Edgeworth-Kuiper Belt objects. *Astron. Astrophys.* **329**, 785–791 (1998)
60. Zank, G.P., Frisch, P.C.: Consequences of a change in the galactic environment of the sun. *Astrophys. J.* **518**, 965–973 (1999)